Aging Clin Exp Res (2016) 28:813–821
DOI 10.1007/s40520-015-0484-3

ORIGINAL ARTICLE

$p15^{INK4b}$ regulates cell cycle signaling in hippocampal astrocytes of aged rats

Fang Wang[1] · Linhong Zhang[1]

Received: 9 August 2015 / Accepted: 19 October 2015 / Published online: 2 November 2015

Abstract
Background and aims Cyclin-dependent kinase inhibitor $p15^{INK4b}$ is thought to be an important player in regulating astrocytic cell cycle. However, little is known with regard to the expression of $p15^{INK4b}$ and its function in hippocampal astrocytes. This study evaluated the expression of $p15^{INK4b}$ and its function during different development stages in hippocampal astrocytes.
Methods In this study, we cultured hippocampal astrocytes from neonatal adult and aged rats. The expression of $p15^{INK4b}$ in neonatal, adult and aged astrocytes was examined. Short interfering RNA (siRNA) was then used to study the functional effects of $p15^{INK4b}$ down-regulation during cell cycle regulation.
Results We found the expression of $p15^{INK4b}$ in hippocampal astrocytes was detectable on postnatal day 7, was expressed at moderate levels in adult mice (9 months old) astrocytes and peaked in aged rat (24 months old) astrocytes. Incubation with siRNA significantly suppressed $p15^{INK4b}$ expression at the mRNA and protein levels in astrocytes. Down-regulation of $p15^{INK4b}$ increased [^{3}H]-thymidine incorporation into DNA and allowed cells to pass the G0/G1-S checkpoint in aged but not in neonatal or adult astrocytes.
Conclusions These observations suggest $p15^{INK4b}$ is expressed at a steady level in neonatal and adult rat hippocampal astrocytes with no effect on cell cycle regulation. Importantly, aged astrocyte cell cycle regulation was significantly affected by high expression levels of $p15^{INK4b}$ suggesting a role for $p15^{INK4b}$ in cell cycle regulation when it is expressed at high but not moderate or low levels in hippocampal astrocytes.

Keywords $p15^{INK4b}$ · Hippocampus · Astrocytes · Cell cycle · Aging

Introduction

Hippocampal astrocytes regulate neurogenesis by instructing stem cells to adopt a neuronal fate, a characteristic important for cognition, behavior, pathophysiology, and recovery after injury [1–3], and are therefore of special interest because of hippocampal involvement in memory and learning [4]. $p15^{INK4b}$ is a member of the cyclin-dependent kinase inhibitor (CKI) family [5]. Previous studies have shown that abnormal expression of $p15^{INK4b}$ resulted in behavioral abnormalities in mice [6] and cell cycle dysregulation in human and murine astrocytes [5]. To date, age-related changes in expression and function of $p15^{INK4b}$ in hippocampal astrocytes during cell cycle regulation have not been investigated.

In this study, we examined $p15^{INK4b}$ expression in hippocampal astrocytes isolated from rats of different ages and studied the effects of loss of $p15^{INK4b}$ on proliferation and cell cycle distribution using small interfering RNA. We show here that $p15^{INK4b}$ is constitutively expressed in the hippocampal astrocytes from neonatal, adult and aged rats, with its peak expression in aged hippocampal astrocytes. Moreover, down-regulation of $p15^{INK4b}$ increased [^{3}H]-thymidine incorporation into DNA and allowed cells to pass the G0/G1-S checkpoint in aged but not neonatal or adult astrocytes.

✉ Fang Wang
wangfangdoc@163.com

[1] Department of Neurology, The Central Hospital of Wuhan, 26 Shengli Street, Wuhan 430014, China

Materials and methods

Animals

Male Wistar rats were used in this study according to protocols approved by the bioethics committee of the central hospital of Wuhan (Permit Number 2011-AR0288). Male rats were assigned into three groups ($n = 8$): neonatal (postnatal day 7), adult (9 months old) and aged (24 months old).

Primary hippocampal astrocyte cultures

Rats were killed and their hippocampi were carefully harvested, minced and trypsinized. Cell suspensions were passed through a 60 pm mesh, pelleted and transferred in complete medium to 75-ml tissue culture flasks. Once cells reached confluency (2–3 weeks), the flasks were shaken overnight at 37 °C and the medium changed the following morning for three consecutive nights. Cells were then trypsinized and cultured for 72 h in 20 mM of cytosine arabinoside to eliminate proliferating cells. These steps were repeated to further eliminate other cell types. These cultures are referred to as passage 1. When cultures reached confluence (1–2 weeks), they were dispersed with trypsin/EDTA and reseeded at approximately 2.3×10^4 cells/cm^2 in 6-well culture dishes for further studies [1, 7, 8].

Small interfering RNA (siRNA) transfection

Transfections were performed in serum-free medium for 6 h at 37 °C with 20 μg Lipofectamine (Invitrogen) in combination with either 150 nM control scrambled siRNA (siRNA ctl) (RiboBio, Guangzhou, China) or a combination of 75 nM siRNA ctl and 75 nM siRNA targeting $p15^{INK4b}$ (siRNA P15) (RiboBio, Guangzhou, China). Hippocampal astrocytes were incubated with serum-free medium for 48 h, and transfected with siRNA. The cells were approximately 60–70 % confluent at the time of transfection. GFP-labeled siRNA targeting $p15^{INK4b}$ (GFP-siRNAp15) (RiboBio, Guangzhou, China) was used to determine transfection efficiency. SiRNA sequences used were as follows: siRNAp15, 5′-GCCCUAUCUAGGAAGACUG-3′ and 5′-CTCAAGGCCGGCGGAGGACC-3′ [9]. To examine siRNAp15 transfection efficiency, GFP-siRNAp15-positive astrocytes were counted under a fluorescence microscope (Axiovert S100, Carl Zeiss, Oberkochen, Germany). Transfection efficiency was determined by quantification of the percentage of GFP-positive cells relative to all cells in culture. To overcome the question of off-target effects during siRNA studies, a second siRNA targeting the $p15^{INK4b}$ gene was designed and transfected into hippocampal astrocytes. The second siRNA sequences were: siRNAp15′, 5′-GCCGATGTCGTAATTCCTATA-3′ and 5′-CTGGAGTGTAGGAATTGACTA-3′. $p15^{INK4b}$ inhibition was quantified by measuring $p15^{INK4b}$ mRNA expression using quantitative real-time PCR. Primers for $p15^{INK4b}$ were 5′-GGAATTCCTGGAAGCCGGCGCAGATC-3′ (forward) and 5′-GCTCTAGAGCGTGTCCAGGAAGCCTTCC-3′ (reverse) (a 190-bp product) [10]. Values were normalized to glyceraldehyde-3-phosphate dehydrogenase (GADPH). Protein level of $p15^{INK4b}$ was also measured by western blotting.

Flow cytometric analysis

To determine the purity of astrocytes, cells were incubated with primary antibodies against glial fibrillary acidic protein (GFAP) (Dako, Carpinteria, CA, USA) and S100beta (Abcam, Cambridge, UK) [11, 12]. This was then followed by incubation with rabbit anti-mouse IgG antibody conjugated with FITC and goat anti-rabbit IgG antibody conjugated with PE (Jackson ImmunoResearch, West Grove, PA, USA). GFAP and S100beta double-positive astrocytes were examined by a flow cytometer (FACSort, BD Biosciences, San Jose, CA, USA). Results were expressed as the percentage of the GFAP/S100beta double-positive cells with respect to total cells.

72 h after siRNAp15 transfection, hippocampal astrocyte cell cycle phase was analyzed by flow cytometry as previously described [13]. Briefly, propidium iodide (0.05 g/l final concentration) was added and the astrocytes were maintained in the darkness at 4 °C until used. The intensity of fluorescence was measured at 560 nm by flow cytometry (FAC Scan, Becton–Dickinson, San Jose, CA, USA). With this experimental procedure, it was possible to analyze both the different phases of the cell cycle and apoptosis by separating cells with a diploid or higher DNA content from those with a hypodiploid DNA content. The stage of the cell cycle was expressed as the percentage of cells in G0/G1 (diploid cells), G2/M (tetraploid cells), and S (intermediate DNA content) phases, respectively. To avoid mistaken results, a program that recognized a single cell with a tetraploid DNA content of an aggregate of two diploid cells was used [13].

[^{3}H]-thymidine incorporation into astrocytes

The rates of astrocytes DNA synthesis were estimated by quantification of the amount of tritium incorporated into the acid-precipitable form after [^{3}H]thymidine incubation, as previously described [13]. Briefly, after 48 h, siRNAp15-transfected astrocytes were treated with [^{3}H]-thymidine at a final concentration of 5 μCi/

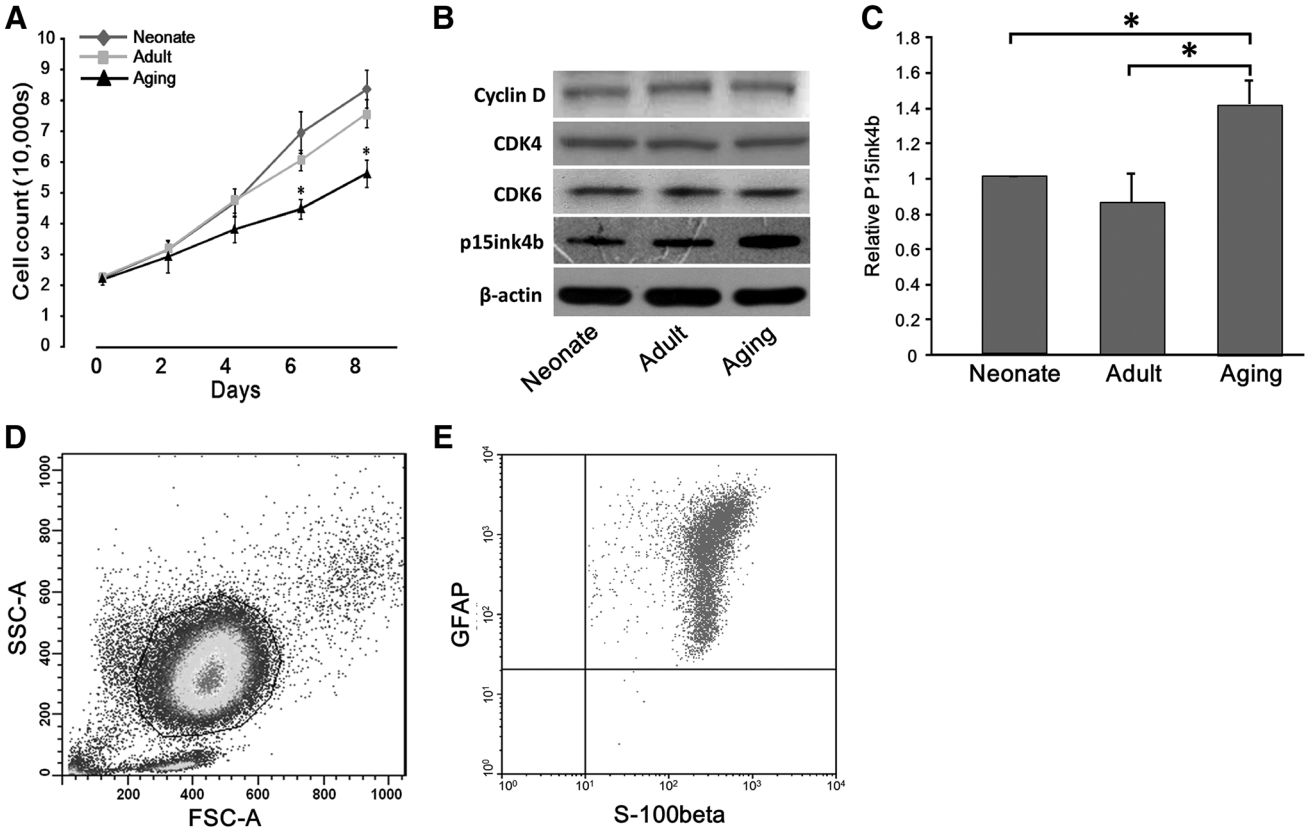

Fig. 1 Isolated astrocytes express varying levels of $p15^{INK4b}$ dependent on stage of development. **a** Cell growth of cultured astrocytes derived from neonatal adult and aged mice. **b** The relative mRNA level for $p15^{INK4b}$ of neonatal, adult or aged astrocytes. **c** The protein levels for $p15^{INK4b}$ of neonatal, adult or aged astrocytes. **d** Freshly isolated astrocytes are shown on the dot plot of forward scatter (*FSC*) versus side angle light scatter (*SSC*). **e** Flow cytometric detection of GFAP and S100beta double-positive cells. Data are mean ± SD ($n = 3$). *$p < 0.05$

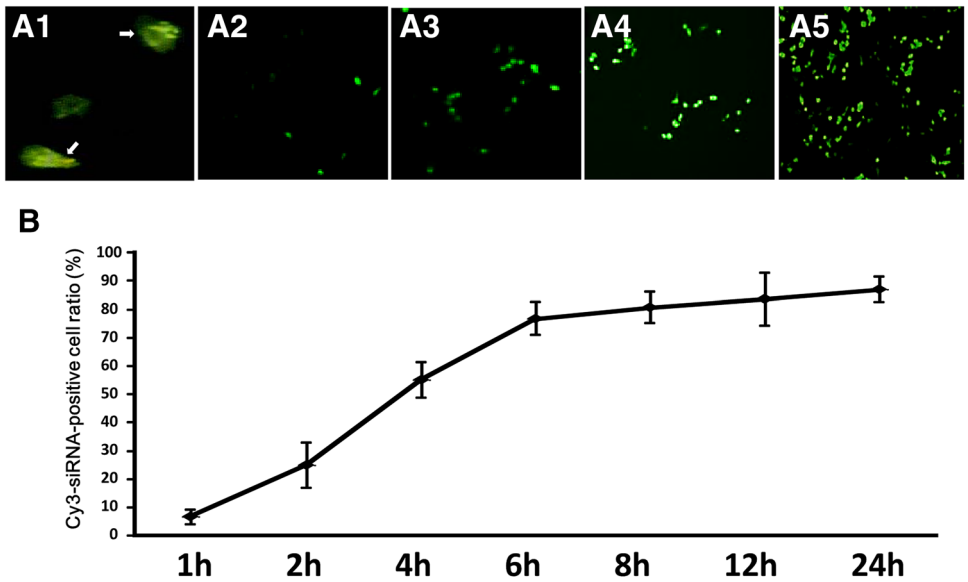

Fig. 2 siRNAp15 transfection in rat astrocytes. **A1**–**A5** Time course of GFAP expression in astrocytes after transfection with siRNAs: **A1** GFP-contained (*green*) astrocytes after 1 h incubation with GFP-siRNAp15. *Arrows* GFP-contained astrocytes (×400). **A2**–**A5** Fluorescent images of GFP-contained astrocytes (×40) at 2, 4, 6 and 24 h post-transfection. **b** GFP-siRNAp15 taken up by astrocytes between 1 and 24 h after transfection

mL for 4 h. Reactions were stopped and cells were incubated with 0.5 M NaOH for 1 h at room temperature and then with 20 % (v/v) cold trichloroacetic acid for 1 h at 4 °C. Washout of the stable isotope was determined at 5, 10, 15, 20, 25 and 30 h after addition of the radioisotope [14]. Results are expressed as percentage change with respect to the [^{3}H]-thymidine incorporated at 5 h.

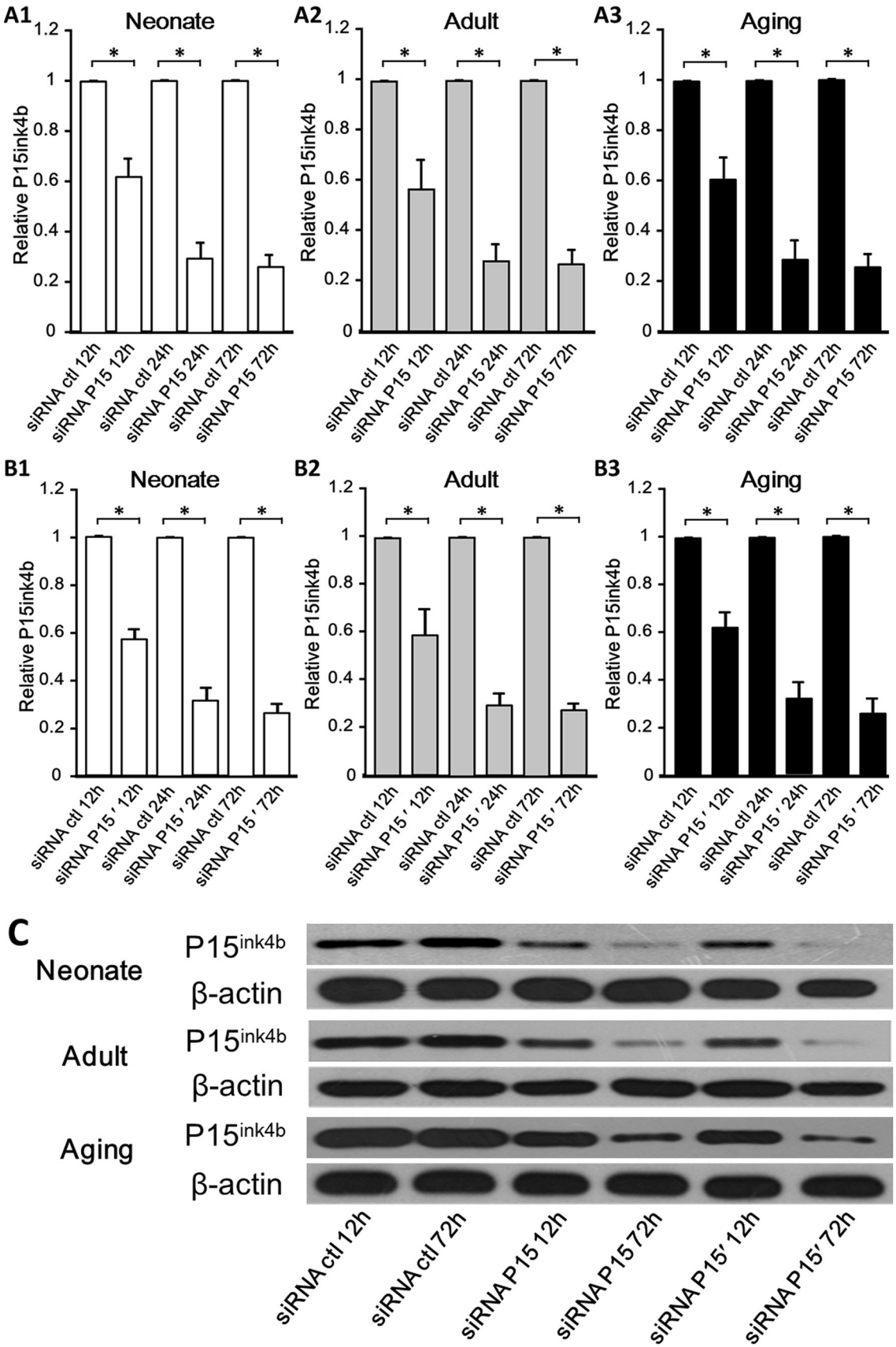
A1
Neonate
A2
Adult
A3
Aging
Relative P15ink4b
1.2
1
0.8
0.6
0.4
0.2
0
*
siRNA ctl 12h
siRNA P15 12h
siRNA ctl 24h
siRNA P15 24h
siRNA ctl 72h
siRNA P15 72h
B1
Neonate
B2
Adult
B3
Aging
siRNA P15 ' 12h
siRNA P15 ' 24h
siRNA P15 ' 72h
C
Neonate
Adult
Aging
P15ink4b
β-actin
siRNA ctl 12h
siRNA ctl 72h
siRNA P15 12h
siRNA P15 72h
siRNA P15' 12h
siRNA P15' 72h

◀**Fig. 3** Inhibition of $p15^{INK4b}$ expression in rat astrocytes. **A1–A3** $p15^{INK4b}$ mRNA was examined by qRT-PCR after siRNAp15 transfection. **B1–B3** $p15^{INK4b}$ mRNA was examined by qRT-PCR after siRNAp15′ transfection. The relative mRNA level for $p15^{INK4b}$ at 12, 24 and 72 h post-transfection was calculated using GAPDH as the internal control. **c** Expression of $p15^{INK4b}$ protein was examined by western blotting at 12 and 72 h post-transfection. Data are mean ± SD ($n = 3$). *$p < 0.05$

Western blot analysis

Hippocampal astrocytes were lysed in RIPA buffer and clarified cytosolic extracts were subjected to SDS-PAGE followed by western blot analysis. Antibodies used for Western blotting include anti-$p15^{INK4b}$ (sc-1429), anti-Cyclin D1 (sc-753), anti-CDK4 (sc-260), and anti-CDK6 (7181). To confirm equal protein loading, membranes were stripped and probed with a 1/10,000 dilution of anti-b-actin antibody.

Statistical analyses

The Student's *t* test was used to compare the difference between two groups and one-way analysis of variance (ANOVA) with post hoc test was used to compare the difference between the three groups. *P* values less than 0.05 were considered statistically significant in all studies. Statistical analyses were performed using SAS software (SAS 9.2, SAS Institute, NC, USA).

Results

In vitro culture of hippocampal astrocytes

To quantify astrocytes growth, suspensions of cells at passage 2 were plated at equal densities of 20,000 cells/well in a six-well plate. The cells from each well were then harvested and counted with a hemacytometer every 2 days. After Days 6 and 8 in culture, the mean number of neonatal astrocytes was 69,777 ± 6807 and 84,000 ± 6245, respectively (Fig. 1a) and the mean number of adult astrocytes was 60,667 ± 3512 and 76,000 ± 4583, respectively. Compared with neonatal and adult astrocytes, the mean number of aged astrocytes was significantly lower at 44,667 ± 3215 and 56,333 ± 4509 for Days 6 and 8 in culture (neonatal vs. aged: $p_{day6} < 0.05$, $p_{day8} < 0.05$; adult vs. aged: $p_{day6} < 0.05$, $p_{day8} < 0.05$). However, no difference of cell growth was found between neonatal and adult astrocytes (all $p > 0.05$).

A cell population of freshly isolated astrocytes gated on a two-dimensional dot plot of forward scatter versus side angle light scatter cells comprised >95 % of the total cells (Fig. 1d). Co-staining of GFAP and S100beta on the dual-color fluorescence histogram clearly showed a double-positive cell population. The percentage of GFAP/S100-beta double-positive cells was >98 % of the gated cells (Fig. 1e). These results clearly demonstrate high purity of cultured astrocytes.

The expression of $p15^{INK4b}$ in hippocampal astrocytes changes with age

The $p15^{INK4b}$ mRNA was detected in neonatal, adult and aged astrocytes (Fig. 1c). The $p15^{INK4b}$ mRNA of aged astrocytes was higher than those of neonatal and adult astrocytes (fold change 1.42 ± 0.14 vs. 1 vs. 0.86 ± 0.17, $p < 0.05$). There was no significant difference in $p15^{INK4b}$ mRNA levels between neonatal and adult astrocytes (fold change 1 vs. 0.86 ± 0.17, $p > 0.05$).

We also examined $p15^{INK4b}$ protein levels in astrocytes (Fig. 1b). Densitometry of western blots was calculated and normalized to β-actin. The $p15^{INK4b}$ protein of aged astrocytes was higher than those of neonatal and adult astrocytes (fold change 1.85 ± 0.17 vs. 0.91 ± 0.22 vs. 1, $p < 0.05$). There was no significant difference in $p15^{INK4b}$ protein levels between neonatal and adult astrocytes (fold change 0.91 ± 0.22 vs. 1, $p > 0.05$). Meanwhile, the protein expressions of cyclin D1, CDK4 and CDK6 were not significantly different between neonatal, adult and aged astrocytes (fold change cyclin D1: 0.92 ± 0.11 vs. 1.02 ± 0.20 vs. 1; CDK4: 0.82 ± 0.12 vs. 0.94 ± 0.17 vs. 1; CDK6: 1.11 ± 0.13 vs. 0.95 ± 0.18 vs. 1; all $p < 0.05$) (Fig. 1b).

Inhibition of $p15^{INK4b}$ induced by siRNA in hippocampal astrocytes

To study the physiological function of $p15^{INK4b}$ in proliferation and cell cycle regulation, we used a siRNA knockdown approach to inhibit the expression of $p15^{INK4b}$. We found that GFP-positive cells (used for transfection efficiency) were observed as early as 60 min after transfection (Fig. 2A1). The number of transfected cells increased constantly up to 6 h and reached a plateau thereafter (Fig. 2A2–A4). At 12 h after transfection, 85 % of the cells had taken up GFP-siRNAp15 (Fig. 2b).

Down-regulation of $p15^{INK4b}$ was confirmed by examining the mRNA and protein levels of $p15^{INK4b}$ (Fig. 3A1–A3). 12 h after siRNA transfection, the mRNA levels of $p15^{INK4b}$ were significantly decreased in neonatal (fold change 0.62 ± 0.07 vs. 1, $p < 0.05$), adult (fold change 0.57 ± 0.12 vs. 1, $p < 0.05$) and aged astrocytes (fold change 0.61 ± 0.09 vs. 1, $p < 0.05$). $p15^{INK4b}$ mRNA was further decreased (fold change: neonate 0.29 ± 0.06 vs. 1; adult 0.28 ± 0.07 vs. 1; aging 0.29 ± 0.08 vs. 1, all $p < 0.05$) 24 h after siRNA transfection. Further, inhibition

of $p15^{INK4b}$ was still observed at 72 h after siRNA transfection (fold change: neonate 0.26 ± 0.05 vs. 1; adult 0.27 ± 0.06 vs. 1; aging 0.25 ± 0.06 vs. 1, all $p < 0.05$). $p15^{INK4b}$ protein was decreased (fold change: neonate 0.49 ± 0.07 vs. 1; adult 0.61 ± 0.11 vs. 1; aging 0.57 ± 0.09 vs. 1, all $p < 0.05$) 12 h after siRNA transfection. Inhibition of $p15^{INK4b}$ was observed at 72 h after siRNA transfection (fold change: neonate 0.22 ± 0.08 vs. 1; adult 0.21 ± 0.07 vs. 1; aging 0.17 ± 0.09 vs. 1, all $p < 0.05$) (Fig. 3c).

To ascertain the specificity of $p15^{INK4b}$ inhibition, we designed a distinct siRNA targeting $p15^{INK4b}$, and transfected the second siRNA (siRNAp15′) using the same protocol. We observed the same inhibition of $p15^{INK4b}$ after siRNAp15′ transfection (Fig. 3B1–B3). The mRNA levels of $p15^{INK4b}$ were significantly decreased 12 h after siRNA transfection in neonatal (fold change 0.56 ± 0.04 vs. 1, $p < 0.05$), adult (fold change 0.58 ± 0.10 vs. 1, $p < 0.05$) and aged astrocytes (fold change 0.61 ± 0.07 vs. 1, $p < 0.05$). $p15^{INK4b}$ mRNA was further decreased (fold change: neonate 0.31 ± 0.03 vs. 1; adult 0.29 ± 0.02 vs. 1; aging 0.31 ± 0.04 vs. 1, all $p < 0.05$) 24 h after siRNA transfection. Further, inhibition of $p15^{INK4b}$ was still observed at 72 h after siRNA transfection (fold change: neonate 0.28 ± 0.02 vs. 1; adult 0.24 ± 0.01 vs. 1; aging 0.25 ± 0.04 vs. 1, all $p < 0.03$). $p15^{INK4b}$ protein was decreased (fold change: neonate 0.53 ± 0.10 vs. 1; adult 0.52 ± 0.09 vs. 1; aging 0.58 ± 0.08 vs. 1, all $p < 0.05$) 12 h after siRNA transfection. Inhibition of $p15^{INK4b}$ was observed at 72 h after siRNA transfection (fold change: neonate 0.23 ± 0.07 vs. 1; adult 0.20 ± 0.09 vs. 1; aging 0.18 ± 0.08 vs. 1, all $p < 0.05$) (Fig. 3c).

$P15^{INK4b}$ knockdown increases [^{3}H]-thymidine incorporation into DNA from aged astrocytes but not from neonatal or adult astrocytes

[^{3}H]-thymidine incorporation into DNA remained unchanged from 5 to 30 h in neonatal, adult or aged astrocytes (Fig. 4a). Compared with the aged astrocytes with normal expression of $p15^{INK4b}$, loss of $p15^{INK4b}$ increased [^{3}H]-thymidine incorporation into DNA in $p15^{INK4b}$ siRNA-treated neonatal, adult and aged astrocytes, respectively, between 10 and 30 h after treatment. Data are mean ± SD ($n = 3$). *$p < 0.05$

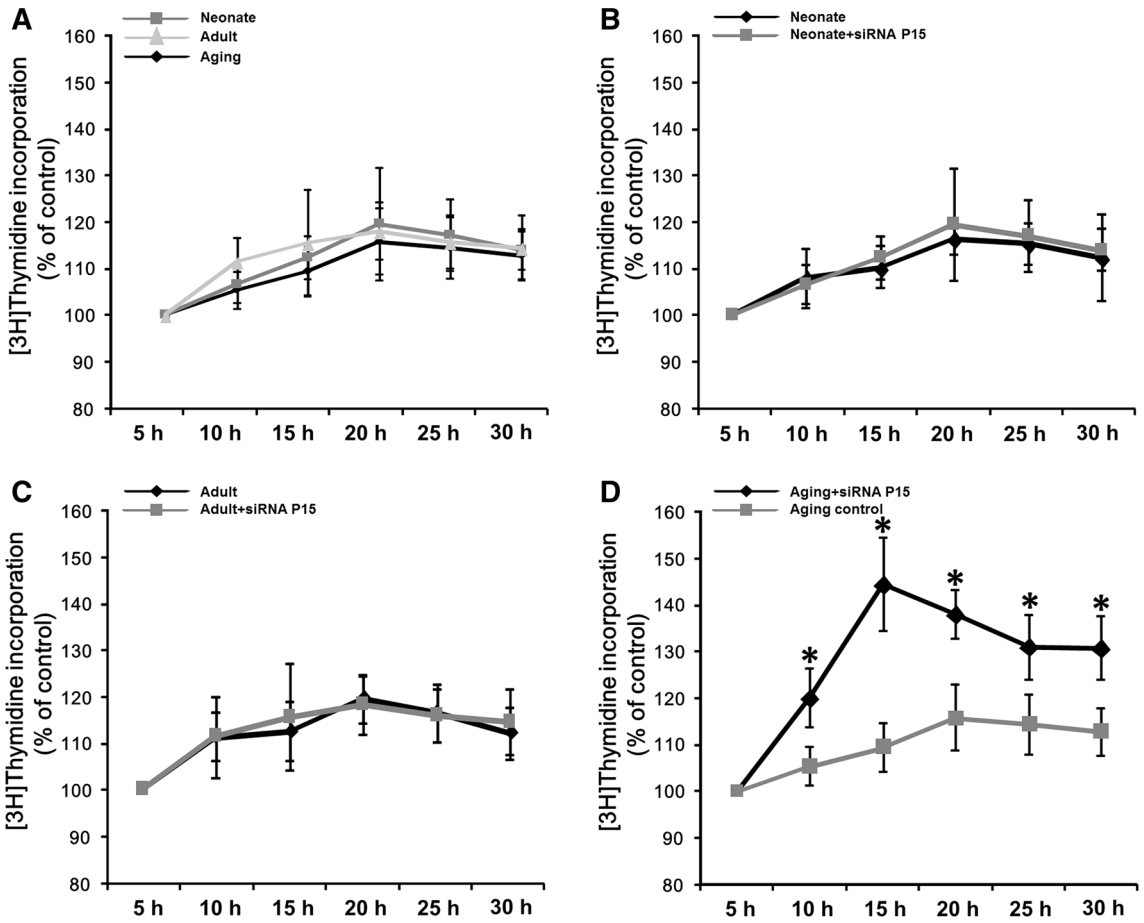

Fig. 4 Effect of down-regulation of $p15^{INK4b}$ on [^{3}H]-thymidine incorporation into DNA from astrocytes. **a** [^{3}H]-thymidine incorporation into DNA between 5 and 30 h after treatment. **b–d** [^{3}H]-

incorporation into the DNA of aged astrocytes at 10 h (percentage change 120 ± 6.2 vs. 105.3 ± 4.0 %, $p < 0.05$), 15 h (percentage change 144.3 ± 10.0 vs. 109.3 ± 5.1 %, *t* test, $p < 0.05$), 20 h (percentage change 138 ± 5.3 vs. 115.7 ± 5.7 %, $p < 0.05$), 25 h (percentage change 131 ± 7 vs. 114.3 ± 6.5 %, $p < 0.05$) and 30 h (percentage change 130.7 ± 6.8 vs. 112.7 ± 5.1 %, $p < 0.05$) (Fig. 4d). However, [^{3}H]-thymidine incorporation into p15^{INK4b}-inhibited neonatal and adult astrocytes remained unchanged between 5 and 30 h (all $p > 0.05$), (Fig. 4b, c).

P15^{INK4b} knockdown promotes G1 to S progression in aged astrocytes but not in neonatal and adult astrocytes

To test this possibility, we transfected hippocampal astrocytes with p15^{INK4b}-specific siRNA and demonstrated a significant inhibition of p15^{INK4b} expression by qRT-PCR. A cell cycle analysis was performed 72 h after the transfection (Fig. 5). We found that loss of p15^{INK4b} in aged astrocytes prevented the G0/G1 arrest (56.4 ± 5.1 % of cells transfected with p15^{INK4b} siRNA were in G0/G1 compared with 73.9 ± 4.16 % of cells transfected with scrambled siRNA, $p < 0.05$). However, down-regulation of p15^{INK4b} increased the percentage of aged astrocytes in S phase from 15.7 ± 2.5 to 26.2 ± 3.5 % when compared with cells transfected with a scrambled siRNA ($p < 0.05$). Down-regulation of p15^{INK4b} did not significantly change the percentage of aged astrocytes in G2/M when compared with controls (12.2 ± 4.5 vs. 17.4 ± 2.9 %, $p < 0.05$) (Fig. 5d).

Cell cycle distribution of neonatal and adult astrocytes was unchanged at 72 h after p15^{INK4b} siRNA transfection (Fig. 5b, c) suggesting that although p15^{INK4b} does not seem to regulate cell cycle progression in neonatal and adult astrocytes, p15^{INK4b} is a key player in the regulation of cell cycle progression in aged astrocytes. No difference in cell cycle distribution was found between the neonatal, adult and aged astrocytes ($p > 0.05$) (Fig. 5a).

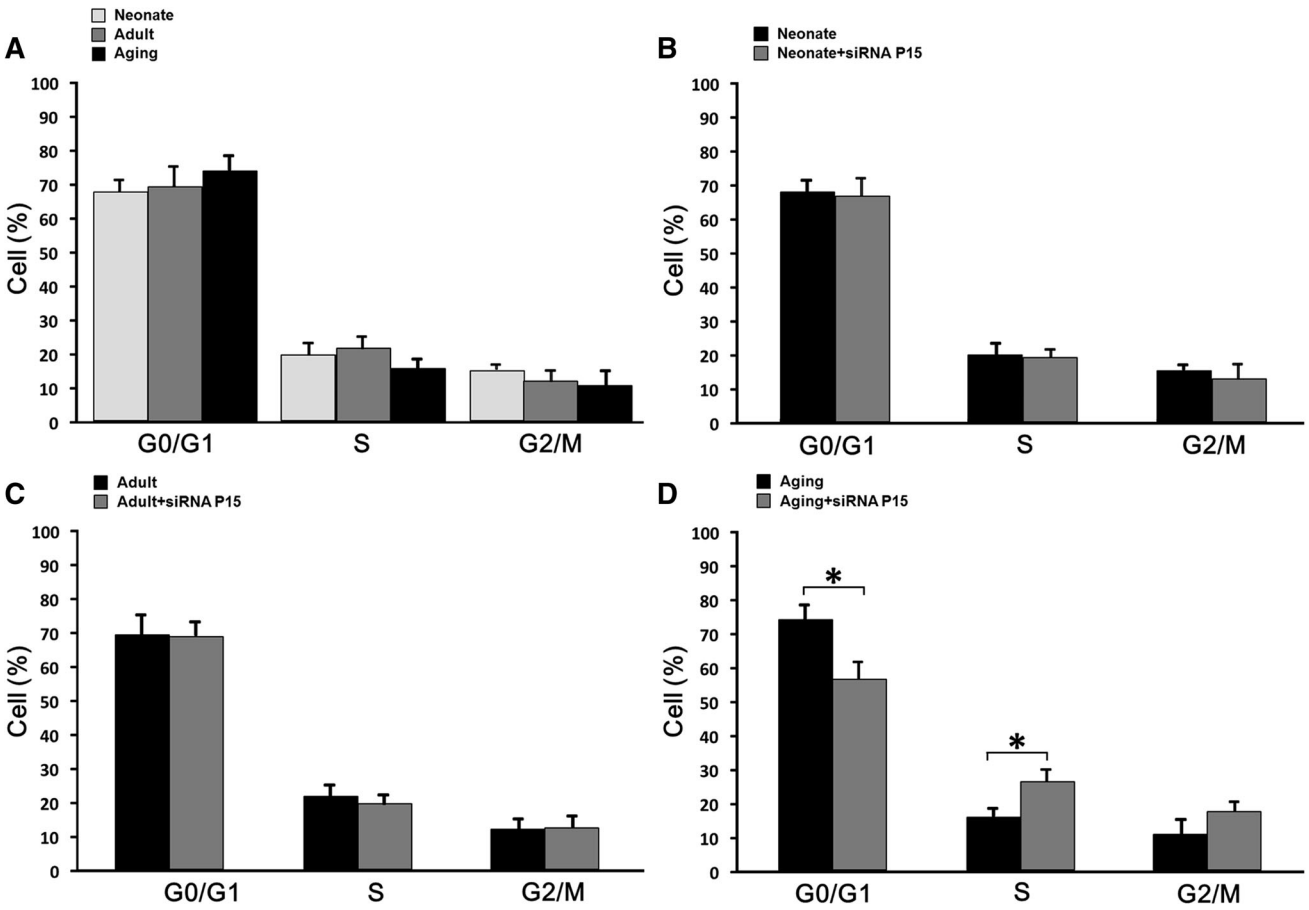

Fig. 5 Effect of down-regulation of p15^{INK4b} on cell cycle distribution of astrocytes. **a** Cell cycle distributions in neonatal, adult and aged astrocytes with normal expression of p15^{INK4b}. **b–d** Cell cycle distribution in neonatal, adult and aged rat astrocytes transfected with p15^{INK4b} siRNA. Data are mean ± SD ($n = 3$). *$p < 0.05$

Discussion

Astrocytes are known to modulate the environment around neurons through their release of a range of neuronal growth factors thus exerting an effect on the neuronal cell cycle in the hippocampus [4]. Recent studies demonstrated that hippocampal astrocytes regulate neural progenitor cell cycle [15] and that the rate of neurogenesis increased greatly after culturing neural stem cells with hippocampal astrocytes suggesting that hippocampal astrocytes provide a unique niche for adult neurogenesis [1].

The rate of neurogenesis is very limited and declines dramatically with age, which is coincident with astrocyte density decline in aged hippocampus [15–18]. Interestingly, astrocytes in aged animals had greater immunoreactivity with GFAP, longer processes, less surface area, and less proliferative ability [16, 19] resulting in decreased proliferation of neural progenitor cells in the aged brain [19]. The exact mechanisms of these astrocyte phenotype and function changes during aging are yet unknown, but are believed to involve changes in cell cycle regulation, which is supported by the observation that genes in cell cycle regulation are differentially expressed by astrocytes during development [20].

Astrocytes cell cycle is strictly controlled by cyclin-dependent kinases (CDK) and its negative regulators, the CKI family [5, 21]. $P15^{INK4b}$ is a member of the CKI family. It binds CDK4/6, frees D cyclins which becomes targeted for ubiquitination and proteosomal degradation, and therefore inhibits the kinase activity of cyclin D-CDK4/6 complexes [22]. Previous studies found that $p15^{INK4b}$ was detectable in the fetal hippocampus and the subsequent loss of $p15^{INK4b}$ expression resulted in behavioral abnormalities in mice [6]. Further, abnormalities and mutations of $p15^{INK4b}$ gene caused loss of stringent growth control of cells [23] and overexpressed $p15^{INK4b}$ resulted in a cell cycle block in G1 phase and inhibited cell proliferation [24].

In this study, we found the $p15^{INK4b}$ mRNA was detectable in neonatal, adult and aged astrocytes with the expression of $p15^{INK4b}$ significantly increased in aged astrocytes. Moreover, we found that the expression of CDK4/6 and cyclin D remained unchanged in neonatal, adult and aged astrocytes. Comparatively high expression of $p15^{INK4b}$ in aged astrocytes would increase cyclin D degradation, and decrease the kinase activity of cyclin D-CDK4/6 complexes. To examine the exact role of $p15^{INK4b}$ in regulating astrocytes cell cycle, we specifically inhibited $p15^{INK4b}$ in astrocytes using silencing RNA. Down-regulation of $p15^{INK4b}$ in astrocytes was observed between 12 and 72 h after siRNA transfection. In aged astrocytes, down-regulation of $p15^{INK4b}$ significantly increased [^{3}H]-thymidine incorporation into DNA and promoted cell cycle progression. However, in neonatal and adult astrocytes, loss of $p15^{INK4b}$ did not change cell proliferation and cell cycle distribution. The data indicate that $p15^{INK4b}$ is a key cell cycle regulator in astrocytes of aged rats, but is apparently not necessary for cell cycle regulation of neonatal and adult astrocytes.

In conclusion, the present study shows $p15^{INK4b}$ is expressed in hippocampal astrocytes obtained from neonatal, adult and aged rats. More importantly, $p15^{INK4b}$ is a key cell cycle regulator in aged astrocytes. These findings increase our knowledge about the expression and function of $p15^{INK4b}$ in rat hippocampal astrocytes and may contribute to a better understanding of the involvement of the CDK inhibitors in the control of neural quiescence in the adult hippocampus.

Acknowledgments We deeply thank Dr. Alyssa Charrier for critical reading and professional revision of our manuscript.

Compliance with ethical standards

Conflict of interest The authors declare that they have no conflict of interest.

Ethical approval All applicable international, national, and/or institutional guidelines for the care and use of animals were followed.

Informed consent Informed consent was obtained from all individual participants included in the study.

References

1. Song H, Stevens C, Gage F (2002) Astroglia induce neurogenesis from adult neural stem cells. Nature 417:39–44
2. Luu P, Sill O, Gao L et al (2012) The role of adult hippocampal neurogenesis in reducing interference. Behav Neurosci 126:384–391
3. Zonis S, Ljubimov V, Mahgerefteh M et al (2013) p21Cip restrains hippocampal neurogenesis and protects neuronal progenitors from apoptosis during acute systemic inflammation. Hippocampus 23:1383–1394
4. Ransom B, Ransom C (2012) Astrocytes: multitalented stars of the central nervous system. Methods Mol Biol 814:3–7
5. Agnihotri S, Wolf A, Picard D et al (2009) GATA4 is a regulator of astrocyte cell proliferation and apoptosis in the human and murine central nervous system. Oncogene 28:3033–3046
6. Albright C, Mar M, Friedrich C et al (2001) Maternal choline availability alters the localization of p15Ink4B and p27Kip1 cyclin-dependent kinase inhibitors in the developing fetal rat brain hippocampus. Dev Neurosci 23:100–106
7. Lin D, Wu J, Holstein D et al (2007) Ca^{2+} signaling, mitochondria and sensitivity to oxidative stress in aging astrocytes. Neurobiol Aging 28:99–111
8. Wilhelm C, Hashimoto J, Roberts M et al (2015) Astrocyte dysfunction induced by alcohol in females but not males. Brain Pathol. doi:10.1111/bpa.12276
9. Fiaschi-Taesch N, Sicari B, Ubriani K et al (2009) Mutant parathyroid hormone-related protein, devoid of the nuclear localization signal, markedly inhibits arterial smooth muscle cell

cycle and neointima formation by coordinate up-regulation of p15Ink4b and p27kip1. Endocrinology 150:1429–1439
10. Joyce N, Harris D, Mello D (2002) Mechanisms of mitotic inhibition in corneal endothelium: contact inhibition and TGF-beta2. Invest Ophthalmol Vis Sci 43:2152–2159
11. Ganz J, Arie I, Ben-Zur T et al (2014) Astrocyte-like cells derived from human oral mucosa stem cells provide neuroprotection in vitro and in vivo. Stem Cells Transl Med 3:375–386
12. Jeong H, Ji K, Min K et al (2014) Astrogliosis is a possible player in preventing delayed neuronal death. Mol Cells 37:345–355
13. Velázquez E, Ruiz-Albusac J, Blázquez E (2003) Glucagon-like peptide-2 stimulates the proliferation of cultured rat astrocytes. Eur J Biochem 270:3001–3009
14. Velázquez E, Santos A, Montes A et al (2006) 25-Hydroxycholesterol has a dual effect on the proliferation of cultured rat astrocytes. Neuropharmacology 51:229–237
15. Miranda C, Braun L, Jiang Y et al (2012) Aging brain microenvironment decreases hippocampal neurogenesis through Wnt-mediated survivin signaling. Aging Cell 11:542–552
16. Lee S, Clemenson G, Gage F (2012) New neurons in an aged brain. Behav Brain Res 227:497–507
17. Ojo J, Rezaie P, Gabbott P et al (2015) Impact of age-related neuroglial cell responses on hippocampal deterioration. Front Aging Neurosci 29:57
18. Zhu J, Mu X, Zeng J et al (2014) Ginsenoside Rg1 prevents cognitive impairment and hippocampus senescence in a rat model of D-galactose-induced aging. PLoS One 9:e101291
19. Bondolfi L, Ermini F, Long J et al (2004) Impact of age and caloric restriction on neurogenesis in the dentate gyrus of C57BL/6 mice. Neurobiol Aging 25:333–340
20. Nakagawa T, Schwartz J (2004) Gene expression patterns in in vivo normal adult astrocytes compared with cultured neonatal and normal adult astrocytes. Neurochem Int 45:203–242
21. Arendt T, Holzer M, Gärtner U (1998) Neuronal expression of cycline dependent kinase inhibitors of the INK4 family in Alzheimer's disease. J Neural Transm 105:949–960
22. Hindley C, Philpott A (2012) Co-ordination of cell cycle and differentiation in the developing nervous system. Biochem J 444:375–382
23. Almeida L, Custódio A, Araújo J et al (2008) Mutational analysis of genes p14ARF, p15INK4b, p16INK4a, and PTEN in human nervous system tumors. Genet Mol Res 7:451–459
24. Fuxe J, Akusjärvi G, Goike H et al (2000) Adenovirus-mediated overexpression of p15INK4B inhibits human glioma cell growth, induces replicative senescence, and inhibits telomerase activity similarly to p16INK4A. Cell Growth Differ 11:373–384